2 Chaos in Laser Systems

Starting from the Maxwell equation in a laser medium based on the model of two-level atoms, we derive the time dependent Maxwell-Bloch equations for field, polarization of matter, and population inversion. Then, we prove that the three differential equations are the same as those of Lorenz chaos. Well above the laser threshold, the laser reaches an unstable point at a certain pump level, which is called second laser threshold. However, only a few real lasers show chaotic dynamics with a second threshold and most other lasers do not have the second threshold, resulting in stable oscillations for the increase of the pump. Stable and unstable oscillations of lasers are related to the scales of the relaxation times for the laser variables. We discuss stability and instability of lasers based on the rate equations and present their classifications from the stability point of view.

2.1 Laser Model and Bloch Equations

2.1.1 Laser Model in a Ring Resonator

The theory of lasers should be treated by the interaction between matter and electro-magnetic field based on quantum mechanics. However, we employ here the semi-classical treatment followed by Haken (1985) and van Tartwijk and Agrawal (1998), which is very easy to understand. Figure 2.1 shows a ring resonator for a laser model with two-level atoms. The model treats only unidirectional wave propagation without considering the backward propagation of light, therefore the development of the equations for the model is very easy. Actual lasers are composed of a Fabry-Perot resonator and have forward and backward waves of light propagations in the laser medium. A few contain a unidirectional ring resonator. The semiconductor laser, which is the main issue of this book, is also basically a Fabry-Perot laser (Abraham et al. 1988). Although the model is not always applicable to real lasers, the description for a unidirectional traveling-wave ring resonator is very simple and the theory can be easily extended to ordinary Fabry-Perot lasers.

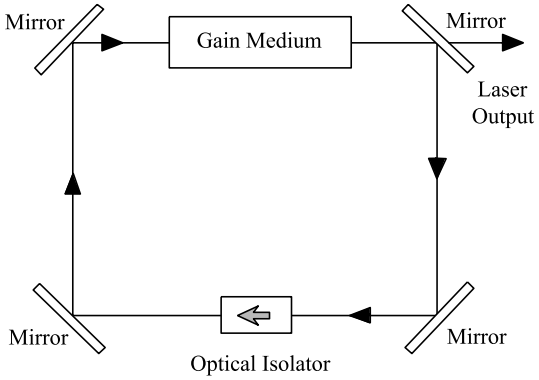

Fig. 2.1. Laser model with ring resonator

The light propagation equation in the laser medium is derived first. The electric field $\boldsymbol{\mathcal{E}}$ (vector field) is written by a time dependent Maxwell equation as

$$\nabla^2 \boldsymbol{\mathcal{E}} - \frac{1}{c^2}\frac{\partial^2 \boldsymbol{\varepsilon}\boldsymbol{\mathcal{E}}}{\partial t^2} = \mu_0 \frac{\partial^2 \boldsymbol{\mathcal{P}}}{\partial t^2} \tag{2.1}$$

where $\boldsymbol{\mathcal{P}}$ is the polarization vector of matter, $\boldsymbol{\varepsilon}$ is the electric permittivity tensor, c is the speed of light in vacuum, and μ_0 is the magnetic permeability in vacuum. Assuming a uniform refractive index of the laser medium and linearly polarized spatial modes for the x and y directions with the propagation for the z axis, the field and the polarization of matter reduce to scalar quantities propagating only to the z direction and (2.1) can be reduced to the following scalar equation:

$$\frac{\partial^2 \boldsymbol{\mathcal{E}}}{\partial z^2} - \frac{\eta^2}{c^2}\frac{\partial^2 \boldsymbol{\mathcal{E}}}{\partial t^2} = \mu_0 \frac{\partial^2 \boldsymbol{\mathcal{P}}}{\partial t^2} \tag{2.2}$$

where η is the refractive index of the laser medium.

The field and the polarization propagate for the z direction with the wavenumber $k = \eta\omega_0/c$ and the angular oscillation frequency ω_0, are then written as

$$\boldsymbol{\mathcal{E}}(z,t) = \frac{1}{2}E(z,t)\exp[\mathrm{i}(kz - \omega_0 t)] + c.c. \tag{2.3}$$

$$\boldsymbol{\mathcal{P}}(z,t) = \frac{1}{2}P(z,t)\exp[\mathrm{i}(kz - \omega_0 t)] + c.c. \tag{2.4}$$

Here, *c.c.* represents the complex conjugate of the preceding terms. $E(z,t)$ and $P(z,t)$ are the amplitudes of the respective variables and are assumed to vary slowly compared with the optical frequency (Slowly Varying Envelope Approximation: SVEA). Neglecting the second order small infinities and sub-

stituting (2.3) and (2.4) into (2.2), we obtain an equation for the amplitudes

$$\frac{\partial E}{\partial z} + \frac{\eta}{c}\frac{\partial E}{\partial t} = \mathrm{i}\frac{k}{2\varepsilon_0 \eta^2} P \tag{2.5}$$

2.1.2 Light Emission and Absorption in Two-Level Atoms

Before deriving the complete form of the propagation equation, we discuss absorption and emission of light from two-level atoms based on the semiclassical quantum theory and, then, derive the Bloch equation. The Hamiltonian $\boldsymbol{\mathcal{H}}_0$ without perturbation for the electric field $\boldsymbol{\mathcal{E}}$, the Hamiltonian $\boldsymbol{\mathcal{H}}$ of the two-level atom is given by

$$\boldsymbol{\mathcal{H}} = \boldsymbol{\mathcal{H}}_0 - \boldsymbol{\mu} \cdot \boldsymbol{\mathcal{E}} \tag{2.6}$$

where $\boldsymbol{\mu} = \boldsymbol{e}\mathbf{r}$ is the moment of the transition between the two levels ($\mathbf{r}$ and $\boldsymbol{e}$ are the position vector and the fundamental electric charge). For the eigenstates $\varphi_j (j = 1, 2)$ of the two levels and the energy of each level as $\hbar\omega_j$ ($\hbar$ being the Planck constant), the interaction between the two levels is written by

$$\langle \varphi_j | \boldsymbol{\mathcal{H}}_0 | \varphi_k \rangle = \hbar\omega_j \delta_{jk} \tag{2.7}$$

where δ_{ij} represents the Kronecker delta. The angular frequency of light emitted or absorbed in the two-level atoms is given by $\omega_\mathrm{A} = \omega_2 - \omega_1$. In the presence of the optical field, the quantum state $|\psi>$ of the two-level atoms is written by the linear addition of the two states as

$$|\psi\rangle = c_1(t)\exp(-\mathrm{i}\omega_1 t)|\varphi_1\rangle + c_2(t)\exp(-\mathrm{i}\omega_2 t)|\varphi_2\rangle \tag{2.8}$$

Substituting the above equation into the Schrödinger equation, the coefficients c_1 and c_2 for the two states are calculated by solving the following coupled equations

$$\frac{\mathrm{d}c_1}{\mathrm{d}t} = \frac{ic_2}{\hbar}\exp(-\mathrm{i}\omega_\mathrm{A} t)\langle \varphi_1 | \boldsymbol{\mu} \cdot \boldsymbol{\mathcal{E}} | \varphi_2 \rangle \tag{2.9}$$

$$\frac{\mathrm{d}c_2}{\mathrm{d}t} = \frac{ic_1}{\hbar}\exp(\mathrm{i}\omega_\mathrm{A}\ t)\langle \varphi_2 | \boldsymbol{\mu} \cdot \boldsymbol{\mathcal{E}} | \varphi_1 \rangle \tag{2.10}$$

These are known as the Bloch equations (1946).

Using the number N_A of atoms in the unit volume, the macroscopic polarization of the medium is defined by

$$\boldsymbol{\mathcal{P}} = N_\mathrm{A}\langle \psi | \boldsymbol{\mu} | \psi \rangle \tag{2.11}$$

From (2.8), the above equation reads as

$$\boldsymbol{\mathcal{P}} = N_\mathrm{A}\{p(t)\mu_{12} + p^*(t)\mu_{21}\} \tag{2.12}$$

Then, the microscopic polarization $p(t)$ for each atom is given by

$$p(t) = c_1^*(t)c_2(t)\exp(-\mathrm{i}\omega_\mathrm{A}t) \tag{2.13}$$

$$\mu_{ij} = \langle\varphi_j|\boldsymbol{\mu}|\varphi_i\rangle \tag{2.14}$$

where $\mu_{ij}(i, j = 1, 2)$ is the moment of the transition from the lower to the upper state or vice versa. Finally, substituting the above equations into (2.9) and (2.10), we obtain the equation for the polarization of atoms

$$\frac{\mathrm{d}p}{\mathrm{d}t} = -\mathrm{i}\omega_\mathrm{A}p + \frac{\mathrm{i}}{\hbar}E\mu_{21}w \tag{2.15}$$

and the distribution $w = |c_2(t)|^2 - |c_1(t)|^2$ for the population inversion of the two-level atoms

$$\frac{\mathrm{d}w}{\mathrm{d}t} = \frac{2}{\mathrm{i}\hbar}E(p^*\mu_{21} - p\mu_{12}) \tag{2.16}$$

2.1.3 Maxwell-Bloch Equations

Rearranging the equations obtained for the field and the polarization and considering the time development of the population inversion in the laser medium, we derive the complete set of laser rate equations, which are the same expressions as those of Lorenz chaos.

Differentiating (2.4) with time and using the relations of (2.12) and (2.15), the macroscopic polarization equation is calculated as

$$\frac{\mathrm{d}P}{\mathrm{d}t} = -\mathrm{i}(\omega_\mathrm{A} - \omega_0)P + \frac{\mathrm{i}\mu^2}{\hbar^2}W[E + E^*\exp\{-2\mathrm{i}(kz - \omega_0 t)\}] \tag{2.17}$$

where $W = N_\mathrm{A}w$ is the macroscopic population inversion and $\mu = |\mu_{12}|$. From (2.16), the equation for the population inversion is given by

$$\frac{\mathrm{d}W}{\mathrm{d}t} = \frac{1}{\mathrm{i}\hbar}[EP^* - EP\exp\{2\mathrm{i}(kz - \omega_0 t)\} - c.c.] \tag{2.18}$$

Since we are concerned with slowly varying variables compared with optical frequency (Rotating-Wave Approximation: RWA), we can omit the terms related to fast oscillation terms of the angular frequency $2\omega_0$ in (2.17) and (2.18) (Milloni and Eberly, 1988).

We need the external pump to lase, so that we add an extra term to (2.18) for lasing in the actual laser. Further, we add the phenomenological terms for the damping oscillations to (2.5), (2.17), and (2.18). The resulting equations,

the Maxwell-Bloch equations, for field E, polarization P, and population inversion W are given by

$$\frac{\partial E}{\partial z} + \frac{\eta}{c}\frac{\partial E}{\partial t} = \mathrm{i}\frac{k}{2\varepsilon_0\eta^2}P - \frac{n}{2T_{\mathrm{ph}}c}E \tag{2.19}$$

$$\frac{\partial P}{\partial t} = -\mathrm{i}(\omega_{\mathrm{A}} - \omega_0)P + \frac{\mathrm{i}\mu^2}{\hbar^2}EW - \frac{P}{T_2} \tag{2.20}$$

$$\frac{\mathrm{d}W}{\mathrm{d}t} = \frac{1}{\mathrm{i}\hbar}(EP^* - E^*P) + \frac{W_0 - W}{T_1} \tag{2.21}$$

where W_0 is the population inversion induced by the pump at the laser threshold. T_{ph}, T_2, and T_1 are the relaxation times of the photons (photon lifetime), the polarization (transverse relaxation), and the population inversion (longitudinal relaxation), respectively. The actual laser exhibits spontaneous emission and, then, statistical Langevin noise terms are added to each equation to explain the noise effects (Pertermann 1988 and Risken 1996). However, statistical noises and irregular chaotic oscillations are of different origins and they can be discussed separately. Chaos is a phenomenon described by deterministic equations, so that such terms are excluded for investigating the pure laser dynamics. Noises are only introduced to account for the effects of laser oscillations when necessary. The Langevin noises will be briefly discussed in Chap. 3.

2.2 Lorenz-Haken Equations

2.2.1 Lorenz-Haken Equations

We have derived the laser equations for field amplitudes and polarization, and population inversion. In the following, we show that these equations are equivalent to Lorenz equations, which describe a model of the convective fluid flow for the atmosphere. Scaling the field E, the polarization P, and the population inversion W in (2.19), (2.20), and (2.21) as $\bar{E} = \sqrt{\varepsilon_0 c\eta/2}E$, $\bar{P} = k/\varepsilon_0\eta^2\sqrt{\varepsilon_0 c\eta/2}P$, and $w = \sigma_{\mathrm{s}}W$ (with $\sigma_{\mathrm{s}} = \mu^2\omega_0 T_2/2\varepsilon_0\hbar c\eta$), and neglecting the term $\partial E/\partial z$ as a small mean field that propagates in the z direction, the Maxwell-Bloch equations are written as follows (Haken 1975);

$$\frac{\mathrm{d}\bar{E}}{\mathrm{d}t} = \mathrm{i}\frac{c}{2\eta}\bar{P} - \frac{1}{2T_{\mathrm{ph}}}\bar{E} \tag{2.22}$$

$$T_2\frac{\mathrm{d}\bar{P}}{\mathrm{d}t} = -(1 - \mathrm{i}\delta)\bar{P} - \mathrm{i}\bar{E}w \tag{2.23}$$

$$T_1\frac{\mathrm{d}w}{\mathrm{d}t} = w_0 - w + \frac{\mathrm{Im}[\bar{E}^*\bar{P}]}{I_{\mathrm{sat}}} \tag{2.24}$$

where $\delta = (\omega_0 - \omega_{\mathrm{A}})T_2$ is the scaled atomic detuning and $I_{\mathrm{sat}} = \hbar^2 c\eta\varepsilon_0/2\mu^2 T_1 T_2$ is the saturation intensity.

In the meantime, Lorenz proposed the differential equations for three variables X, Y, and Z as a model of atmospheric flow (Rayleigh-Bénard configuration) and proved the existence of chaos in the system (Lorenz 1963). Using chaotic parameters Σ, R, and β, the Lorenz equations are written as

$$\frac{\mathrm{d}X}{\mathrm{d}t} = -\Sigma(X - Y) \tag{2.25}$$

$$\frac{\mathrm{d}Y}{\mathrm{d}t} = RX - Y - XZ \tag{2.26}$$

$$\frac{\mathrm{d}Z}{\mathrm{d}t} = -\beta Z + XY \tag{2.27}$$

Lorenz suggested that systems described by nonlinearly coupled differential equations with three variables are candidates for chaotic systems. By normalizing the variables as $x = \sqrt{b/I_{\mathrm{sat}}}\bar{E}$, $y = (\mathrm{i}cT_{\mathrm{ph}}/\eta)\sqrt{b/I_{\mathrm{sat}}}\bar{P}$, and $z = (w_0 - w)cT_{\mathrm{ph}}/\eta$, and replacing time by $t/T_2 \to t$, the Maxwell-Bloch equations in (2.22)–(2.24) are written as

$$\frac{\mathrm{d}x}{\mathrm{d}t} = -\sigma(x - y) \tag{2.28}$$

$$\frac{\mathrm{d}y}{\mathrm{d}t} = -(1 - \mathrm{i}\delta)y + (r - z)x \tag{2.29}$$

$$\frac{\mathrm{d}z}{\mathrm{d}t} = -bz + \mathrm{Re}[x^* y] \tag{2.30}$$

where $\sigma = T_2/2T_{\mathrm{ph}}$, $b = T_2/T_1$, and $r = w_0 cT_{\mathrm{ph}}/\eta$. It is easily proved that the above three equations are the same as those of the Lorenz model and lasers described by two-level atoms are essentially the same chaotic system as the convective fluid in the atmospheric flow. Thus, (2.28)–(2.30) are called the Lorenz-Haken equations.

2.2.2 First Laser Threshold

A laser oscillation starts when the population inversion exceeds a certain level, namely the pumping threshold. The laser threshold can be calculated from (2.28)–(2.30) based on the linear stability analysis. The linear stability analysis, which applies small perturbations on the steady-states of the laser variables, is frequently used for obtaining the stability conditions. Assuming the stable solutions in (2.28)–(2.30) as x_{s}, y_{s}, and z_{s}, and applying small perturbations on the steady-state values, we write the time developments of the variables as $x(t) = x_{\mathrm{s}} + \delta x(t)$, $y(t) = y_{\mathrm{s}} + \delta y(t)$, and $z(t) = z_{\mathrm{s}} + \delta z(t)$, where $\delta x(t)$, $\delta y(t)$, $\delta z(t)$ are small perturbations. Substituting these values into (2.28)–(2.30), we obtain the following differential equations for the perturbations

$$\frac{\mathrm{d}\delta x}{\mathrm{d}t} = -\sigma(\delta x - \delta y) \tag{2.31}$$

$$\frac{\mathrm{d}\delta y}{\mathrm{d}t} = -(1 - \mathrm{i}\delta)\delta y - (r - \delta z)\delta x \tag{2.32}$$

$$\frac{\mathrm{d}\delta z}{\mathrm{d}t} = -b\delta z + \mathrm{Re}[\delta x^* \delta y] \tag{2.33}$$

We can neglect the second small infinities such as $\delta z \delta x$ and $\delta x^* \delta y$, thus the equations are linearized.

When we put the time developments of the variables as $\delta h = \delta h_0 \exp(\gamma t)$ $(h = x, y, z)$, the laser is stable for solutions of negative real parts of γ. On the other hand, it is unstable for solutions of positive real parts and the solutions diverge to infinities for the time development. Substituting the time developments $\delta h = \delta h_0 \exp(\gamma t)$ into (2.31)–(2.33), we obtain the following characteristic relation for the non-trivial solutions

$$\begin{vmatrix} \gamma + \sigma & -\delta & 0 \\ -r & \gamma + 1 - \mathrm{i}\delta & 0 \\ 0 & 0 & \gamma + b \end{vmatrix} = 0 \tag{2.34}$$

The real parts of the solutions in the above equations represent the measure for stability or instability of the solutions and the imaginary parts denote the oscillation frequencies of the corresponding solutions. Since $b = T_2/T_1$ is positive, one of the solutions $\gamma = -b$ is a stable solution with uniform convergence. The other solutions are calculated by solving the following equations

$$\gamma^2 + (\sigma + 1 - \mathrm{i}\delta)\gamma - \sigma(r - 1 + \mathrm{i}\delta) = 0 \tag{2.35}$$

When the pumping r reaches a certain value, the laser exceeds the threshold and laser oscillation starts. Above the threshold, the solutions of the imaginary parts are enough to take into account. Putting the form of the solutions as $\gamma = i\Omega$ and substituting it into (2.35), we obtain the laser threshold from the conditions having zero values for the real and imaginary parts of (2.35) as

$$r_{\mathrm{th}}^{(1)} = 1 + \frac{\delta^2}{(\sigma + 1)^2} \tag{2.36}$$

For the laser oscillation, there is an accompanying frequency $\nu = \Omega/2\pi$ that corresponds to the solution of the imaginary part for the characteristic equation. Using the threshold, the frequency is given by

$$\nu_{\mathrm{R}} = \frac{\sigma}{2\pi}\sqrt{r_{\mathrm{th}}^{(1)} - 1} \tag{2.37}$$

The frequency ν_{R} is known as the relaxation oscillation frequency. When the detuning δ is zero, the threshold is $r_{\mathrm{th}}^{(1)} = 1$ or $w_0 = \eta/cT_{\mathrm{ph}}$, as expected. The extra term in the threshold in (2.36) is the increase of the threshold, which compensates the loss due to the detuning. As we discuss in the following section, there is another threshold that is called second laser threshold. Therefore, $r_{\mathrm{th}}^{(1)}$ is called first laser threshold.

2.2.3 Second Laser Threshold

Laser oscillation starts above the first threshold and shows a stable output power at a certain pump. Here, we again apply linear stability analysis for the laser operation. As we are considering the oscillation above the threshold, the field and the polarization vary with time at the same optical frequency for the steady-state values of x_s, y_s, and z_s. Assuming the difference of the angular detuning frequency $\Delta\omega$ between the laser oscillation and the internal cavity frequencies and the phase fluctuation ϕ_s of the complex field, we put the forms of the steady-state solutions as

$$x_\mathrm{s} = x_0 \exp\{-\mathrm{i}(\Delta\omega_\mathrm{s} t + \phi_\mathrm{s})\} \tag{2.38}$$

$$y_\mathrm{s} = y_0 \exp(-\mathrm{i}\Delta\omega_\mathrm{s} t) \tag{2.39}$$

$$z_\mathrm{s} = z_0 \tag{2.40}$$

where $x_0 = \sqrt{bz_0}$, $y_0 = \sqrt{r_\mathrm{th}^{(1)} bz_0}$, $z_0 = r - r_\mathrm{th}^{(1)}$, $\Delta\omega_\mathrm{s} = -\delta\sigma/(\sigma+1)$, and $\tan\phi_\mathrm{s} = \delta/(\sigma+1)$. The laser output power is given by the square of x_0 and reads

$$x_0^2 = b\left(r - r_\mathrm{th}^{(1)}\right) \tag{2.41}$$

This is the well-known result that the laser output power linearly increases with the increase of the pump r well above the threshold $r_\mathrm{th}^{(1)}$.

For a pump below the laser threshold, the laser does not reach laser oscillation and it only exhibits a faint light output due to spontaneous emission, thus the laser is also under another stable condition. For the increase of the pump r over the threshold, whether the laser output power increases with the increase of the pump or not? In actual fact, there are nonlinear effects, such as saturation of gains of the laser material, to limit the optical output power. The effects also induce the change of laser parameter values describing the laser rate equations. Of course, what we are considering is not such effects, but the nonlinear effects intrinsically involved in the laser rate equations in (2.28)–(2.30). Here, consider the unstable phenomena induced by the increase of the pump r for these equations. For this purpose, we again employ the linear stability analysis for (2.38)–(2.40) near the steady-state values for the variables. The procedure is almost the same as the previous calculations. For simplicity, we calculate the stability solutions for the condition $\delta = 0$ (zero detuning condition). After some calculations, the same as the derivation for (2.35), the characteristic equation reads

$$\gamma^3 + a_2\gamma^2 + a_1\gamma + a_0 = 0 \tag{2.42}$$

where $a_2 = \sigma + b + 1$, $a_1 = b(\sigma + r)$, and $a_0 = 2b\sigma(r-1)$. The stability solutions are calculated by solving the above equation.

At the threshold of the stable solution, the variable γ is purely imaginary, and it is assumed as $\gamma = i\Omega$. From the comparison between the real and imaginary parts for the solution, we obtain the threshold as

$$r_{\text{th}}^{(2)} = \frac{\sigma(\sigma + b + 3)}{\sigma - b - 1} \tag{2.43}$$

Over the pump r exceeding the threshold $r_{\text{th}}^{(2)}$, the laser gets unstable states and exhibits irregular oscillations of chaos via Hopf bifurcations (see Appendix A.1). In actual evolution processes for bifurcations, there are various routes to chaos, for example, chaos follows immediately after period-1 oscillation (quasi-period-doubling bifurcation). The other example is that instability to chaos follows after intermittent oscillations like spiky irregular oscillations. The details of routes to chaos in semiconductor lasers will be demonstrated in the following chapters. The threshold $r_{\text{th}}^{(2)}$ is called second threshold to distinguish it from the first laser threshold $r_{\text{th}}^{(1)}$. For example, for the conditions of $T_2 >> T_1$, $b \approx 0$, and $\sigma = 2(T_2 = 4T_{\text{ph}})$, the threshold value is equal to $r_{\text{th}}^{(2)} = 10$ and it is much higher than the first threshold $r_{\text{th}}^{(1)} = 1$ without detuning. Actual unstable lasers have the second threshold values around tens to one hundred.

The typical frequency of the irregular pulsing can also be calculated from the characteristic equation for the pure imaginary part value of the variable Γ, and it is given by

$$\nu_{\text{R2}} = \frac{1}{2\pi}\sqrt{b\left(\sigma + r_{\text{th}}^{(2)}\right)} \tag{2.44}$$

For the existence of the second threshold, the condition of $\sigma > b + 1$ must be satisfied from (2.43). This is known as the bad-cavity condition of a laser that gives rise to unstable laser oscillations. The bad-cavity condition is rewritten by using the actual time constants as follows;

$$\frac{1}{2T_{\text{ph}}} > \frac{1}{T_2} + \frac{1}{T_1} \tag{2.45}$$

Namely, the bad-cavity of a laser oscillation is a lossy and dissipative system for photons having a low quality factor Q of the resonator. Further discussion of the bad-cavity conditions and instabilities above the second laser threshold can be found in the reference (van Tartwijk and Agrawal 1998). Equations (2.43) and (2.44) were derived for the condition of zero frequency detuning $\delta = 0$. For non-zero detuning $\delta \neq 0$, the analysis becomes much more complex, but the expression for this case has been given and almost the same order of the second laser threshold $r_{\text{th}}^{(2)}$ has been obtained (Mandel and Zeghlache 1983, Zeghlache and Mandel 1985, and Ning and Haken 1990).

2.3 Classifications of Lasers

2.3.1 Classes of Lasers

We have taken into consideration all of the time constants for the field, the polarization of matter, and the population inversion in the laser rate equations. The second laser threshold has been calculated for the inclusions of these parameters. However, lasers do not always show instabilities and chaotic behaviors with increased pumping, and most lasers are indeed stable. Only few lasers emitting infrared lines exhibit chaotic oscillations. For stability and instability of lasers, we have assumed the model of a ring laser with two-level atoms. On the other hand, most lasers in practical use are modeled by three- or four-level atoms. Therefore, lasers must be modeled by these in a strict sense and some modifications may be required for the above derivations. However, the results derived for the two-level atoms can here be extended to three- or four-level atoms and still be applicable for the discussion of the stability and instability for practical lasers.

Even for the same material, the laser may have several oscillation lines. In such a case, the laser has a different gain for each line and has different time constants for the relaxation oscillations depending on the oscillation frequency. Therefore, a laser with a certain material may be stable for a certain oscillation line and have no second threshold, while it may be unstable and have the second threshold for another line. The stability and instability of lasers intrinsically involved in laser rate equations are classified according to the scales of time constants for the relaxation oscillations T_{ph}, T_2, and T_1 introduced in Sect. 2.2.1. Namely, one or two of the time constants among the three in the differential equations may be adiabatically eliminated and one or two of the laser rate equations are enough to describe actual laser operations. Depending on the scales of the time constants, the stabilities of lasers are classified into the following three classes; class A, B, and C lasers (Arrechi et al. 1984a, b and Tredicce et al. 1985).

2.3.2 Class C Lasers

When the time constants of the relaxations are of the same order, we must consider all of the Lorenz-Haken differential equations. As already discussed, the laser oscillation starts at the first threshold with stable light output for a certain pump and it reaches the second laser threshold for the increase of the pump. Over pumping above the second threshold in the bad-cavity condition with low Q factor, the laser shows unstable oscillation like irregular pulsations and chaotic oscillations. According to the classifications of laser operations by Arecchi et al. (1984a), these lasers are called class C lasers. Class C lasers are generally infrared lasers and far-infrared lasers are almost classified into class C. This is originated from the fact that the three time constants of the relaxation oscillations for the field, the polarization of matter, and the

population inversion tend to be the same order. Examples of class C lasers are NH_3 lasers (Weiss et al. 1985 and Hogenboom et al. 1985), Ne-Xe lasers (3.51 μm line) (Casperson 1978 and Special issue J. Opt. Soc. Am B 1985), and He-Ne lasers at 3.39 μm line (Weiss and King 1982, and Weiss et al. 1983). Though He-Ne lasers operating at infrared lines are class C lasers, He-Ne lasers at visible oscillations are categorized into a different class because the constants of the polarization and the population inversion have different time scales from those of the infrared operations. In general, these class C lasers do not have any commercial application.

Figure 2.2 is an example of experimentally observed chaotic waveforms in an infrared He-Ne laser at 3.39 μm oscillation (Weiss 1983). The bad-cavity condition was realized by tilting the angle of one of the mirrors in the laser resonator. A stable laser state **a** evolves into unstable oscillations **b**–**d** to chaotic state **e** with the increase of the mirror tilting angle. Figure 2.3 shows the oscillation spectra of the laser corresponding to period-doubling bifurcations to chaos for the increase of the mirror tilting angle. Figure 2.4

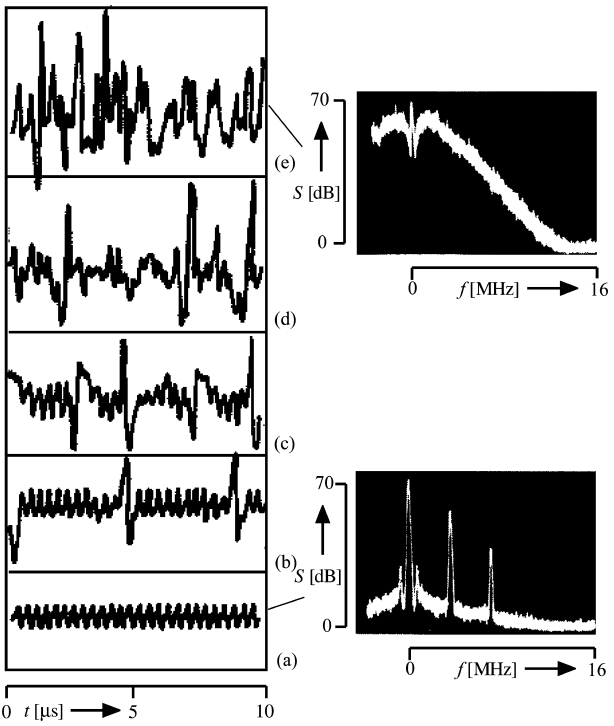

Fig. 2.2. Experimentally observed chaotic time series in an infrared He-Ne laser. Stable oscillation state (a) to chaotic state **e**. One of the mirrors in the laser cavity is tilted and the bad-cavity condition is realized (after Weiss CO, Godone A, Olafsson A (1983); © 1983 APS)

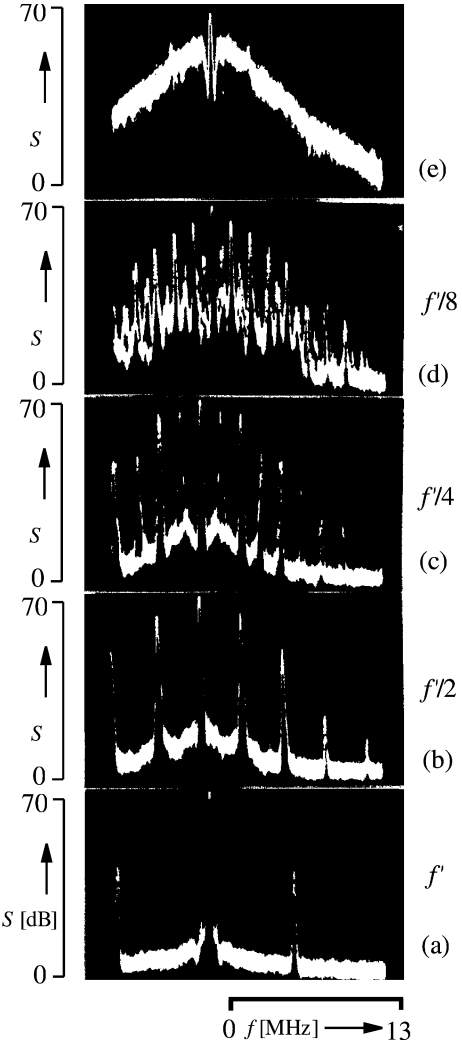

Fig. 2.3. Experimentally observed optical power spectra in an infrared He-Ne laser for period-doubling route to chaos. Tilting of one of the resonator mirrors leads to oscillations to **a** period-1, **b** period-2, **c** period-4, **d** period-8, and **e** chaos (after Weiss CO, Godone A, Olafsson A (1983); © 1983 APS)

is another experimental example of chaos showing pulsation instability in a Xe laser at 3.51 μm oscillation (Casperson 1978). With increasing pump, period-1 pulsation at first appears in Fig. 2.4a and the laser switches to period-2 pulsation in Fig. 2.4b. Thus, routes to chaos are not unique and depend on systems and parameters.

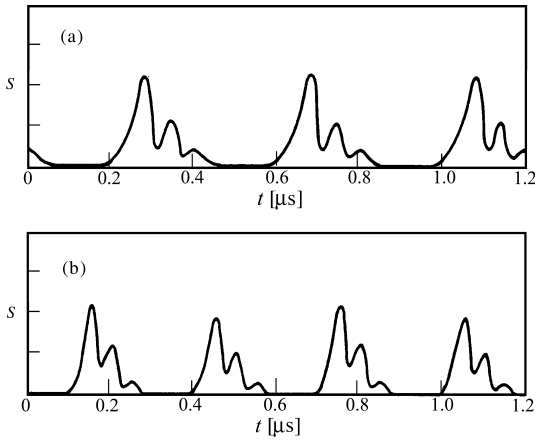

Fig. 2.4. Experimental plots of pulsation instabilities in an Xe laser at 3.51 μm oscillation for **a** period-1 pulsation at a discharge current of 40 mA and **b** period-2 pulsations at a discharge current of 50 mA (after Casperson LW (1978); © 1978 IEEE)

2.3.3 Class B Lasers

The time constant T_2 of the polarization of matter (transverse relaxation) is small enough compared with the other time constants, i.e., T_{ph}, $T_1 \gg T_2$, the differential equation for the polarization is adiabatically eliminated and we obtain for the representation of the polarization in (2.32) (Haken 1985)

$$y = \frac{r - z}{1 - \mathrm{i}\delta} x \tag{2.46}$$

Then, the laser rate equations can be described by the two differential equations for the field x and the population inversion z. These lasers are called class B lasers and they are stable in nature, since the lasers have the first threshold but do not have the second threshold. The electric field is complex and the complex field equation can be split into two differential equations, the amplitude and phase equations. However, the phase equation has no effect on other variables, so that these systems can still be characterized by two differential equations. Therefore, class B lasers are intrinsically stable.

However, they are easily destabilized by the introduction of external perturbations, resulting in the addition of extra degrees of freedom. If the equations for the field amplitude and the phase couple with each other through a perturbation, the laser must be described by the rate equations coupled with three variables. A laser coupled with three variables becomes a chaotic system and shows instabilities. Examples of external perturbations are modulation for the accessible laser parameters, external optical injection, and optical self-feedback from external optical components. Semiconductor

laser, which is the main topic of this book, are classified into class B laser, as discussed later. Indeed, semiconductor lasers are easily destabilized and show chaotic behaviors by external perturbations, such as external optical feedback (van Tartwijk and Agrawal 1998 and Ohtsubo 2002a). One of the typical features of class B lasers is a relaxation oscillation of the laser output that is observed for a step time response when the population inversion does not follow the photon decay rate, i.e., $T_1 > T_{\rm ph}$. Many lasers are classified into class B lasers and other examples are CO_2 lasers and solid state lasers including fiber lasers.

2.3.4 Class A Lasers

When the lifetime of photons in a laser medium is large enough compared with the other time constants of the relaxations, i.e., $T_{\rm ph} \ll T_1, T_2$, the differential equations for the polarization of matter and the population inversion are adiabatically eliminated. In the same manner as class B lasers, the steady-state population inversion is given by (Haken 1985)

$$z = \frac{1}{b}\mathrm{Re}[x^* y] \ . \tag{2.47}$$

Then, the laser oscillation is only described by the differential equation for the field. Lasers satisfying the relations are called class A lasers and they are the most stable lasers with a high Q factor among the three classes. Even for class A lasers, they may be destabilized and show chaotic behaviors by external perturbations with two or more extra degrees of freedom as described in class B lasers. Visible He-Ne lasers, Ar-ion lasers, and dye lasers are examples of class A lasers.

http://www.springer.com/978-3-540-72647-0

Semiconductor Lasers
Stability, Instability and Chaos
Ohtsubo, J.
2008, XVIII, 475 p. 169 illus., Hardcover
ISBN: 978-3-540-72647-0